Influence of band non-parabolicity on the quantized gate capacitance in δ-doped MODFED of III–V and related materials

Sitangshu Bhattacharya,[a] Surya Shankar Dan, and Santanu Mahapatra
Nanoscale Device Research Laboratory, Centre for Electronic Design and Technology, Indian Institute of Science, Bangalore 560 012, India

(Received 8 June 2008; accepted 29 July 2008; published online 1 October 2008)

We have investigated analytically the influence of band non-parabolicity on the quantized gate capacitance in *n*-channel inversion layers of $Al_xGa_{1-x}As|GaAs$, $In_{1-x}As_xSb|InSb$, and $In_{1-x}Al_xAs|In_{1-x}Ga_xAs_yP_{1-x}$ δ-doped modulation field effect devices, whose channel electrons obey the three, two, and the parabolic energy band models of Kane. The quantized gate capacitance has been investigated by including the effects of electric subbands under quantum mechanical treatment on GaAs, InSb, and $In_{1-x}Ga_xAs_yP_{1-y}$ lattices matched to InP as channel materials. The oscillatory dependence of the quantized gate capacitance as a function of surface electric field and gate bias signatures directly the two-dimensional quantum confinement of the carriers. The influence of the band non-parabolicity of the confined carriers significantly influences the value of the gate capacitance. The result of the gate capacitances for the parabolic energy band model forms a special case of our generalized theoretical formalism. © *2008 American Institute of Physics*. [DOI: 10.1063/1.2986154]

I. INTRODUCTION

An enormous range of important applications concerning field effect transistors (FET) in the quantum regime, together with a rapid increase in computing power, have generated much interest in exploiting the physical and electronic properties of nanoscale transistors made up of compound semiconductors. Examples of such applications includes various quantum wire FET,[1] quantum dot transistors,[2] quantum resistors,[3] resonant tunneling diodes,[4] quantum switches,[5] quantum sensors,[6] quantum logic gates,[7] optical modulators,[8] optical switching systems,[9] etc. The rapid downscaling in geometrical dimensions of electronic materials using improved technological processes[10–14] has lead to the invention of modulation doping[15] (MOD) in heterostructures. The controlled growth of multiple epitaxial heterostructures in subnanoscale regime, made up of III–V compound semiconductors, with excellent compositional and thickness control has been possible recently.[16–18] In heterostructures such as quantum wells, the reduction in the *k*-space symmetry of the carriers along one direction can be defined as the one-dimensional (1D) carrier confinement by an infinitely deep 1D potential well, leading to quantized size effect of the wave vectors allowing two-dimensional (2D) electron transport phenomena, not exhibited in bulk semiconductors.

The III–V quantum well field effect transistors such as AlGaN/GaN,[19,20] AlGaAs|GaAs, AlInAs|GaInAs,[21,22] InGaAs|InAlAs,[23,24] etc. came into picture due to very high electron mobility and conductivity[25,26] compared to their corresponding bulk systems. This signatures the increased transistor drive current at both low and high drain bias, which are very important for high speed logic applications. The III–V MODFET also exhibits a high reduction in gate and energy delay product relative to the silicon MOSFETs.[27] In MODFET devices, the carrier concentration within a semiconductor layer can be increased significantly without the introduction of dopant impurities.[6] As it is, a conventional doping technique is important for increasing the free carriers and conductivity in a semiconductor but it comes at the cost of increased ionized impurity scattering, thus, reducing the carrier mobility, leading to reduction in the operation speed of the device. MODFED provides an extremely important alternative to this problem. In a MODFED, the free carrier concentration can be increased significantly without reducing the mobility by spatially separating them from the dopants, thus, minimizing the scattering. Due to such increased value of mobility, MODFETs are usually fabricated from III–V compound semiconductors and are being recently studied in the literature.[28–33] The experimental demonstration of the dislocation free $GaAs/In_{0.15}Ga_{0.85}As$ (on GaAs) MODFET by Rosenberg *et al.*[34] has lead such device to find extensive applications in high-frequency and power circuits,[35] microwave circuits,[36] data processing,[37] terahertz electronics,[38] ultrahigh speed transistors,[39,40] etc.. The δ-doped GaAs MODFET have been reported to have many advantages, such as higher mobility of the carriers, high breakdown voltage, and easy control of threshold voltage and drain current.[41] Such doping profiles also provide significant improvement in linear operation of the device in ac regime.[42,43] This distribution of the carrier profile of the dopant atoms can be well represented by using the Gaussian distribution function.[44] It should be noted that the carrier statistics of the two dimensional electron gas (2DEG) formed at the interface of the heterojunction in a δ-doped MODFED depends strongly on the band structure of the confined carriers and the applied electric field. Considering an undoped substrate material, the *n*-inversion channel so formed may be approximated by a triangular potential well.[45–47] For a channel made of III–V and related ternary material, the conduction electrons obey

[a]Electronic mail: isbsin@yahoo.co.in.

the three, two, and the parabolic energy band models of Kane.[48,49] Due to the introduction of band non-parabolicity, the density of states becomes a function of the electron energy and hence the quantization effects in gate capacitance will be of much interest to investigate. In MODFETs, the gate being an integral part of the heterogeneous system, however, makes it differ from the more conventional structures with respect to the gate capacitance-voltage characteristics. Thus, an accurate accounting of such characteristics is of paramount importance at both low and high temperatures. The application of a strong electric field at the channel leads to 2DEG, which changes the electron dispersion relation of the carriers. As a consequence, the drain saturation current changes, which may reflect serious consequences on the transconductance and current driving capabilities of the concerned device.

What follows, in Sec. II A of the theoretical background, the gate capacitance of δ-doped MODFED at high and low temperatures have been formulated under externally applied electric field following the carrier statistics of the 2DEG formed in the n-channel inversion layers of III–V and related materials as substrates, whose conduction electrons obey the three band model of Kane. The density-of-states function in such condition has been formulated by incorporating the spin-orbit interaction and the band non-parabolicity parameter.[48] In Sec. II B, all the corresponding cases following. Sec. II A has been investigated by considering the simplified two band model of Kane, and under certain limiting conditions, all the corresponding expressions of Sec. II B form special cases of Sec. II A. In Sec. II C, the same has been studied by considering the well known parabolic energy band model of the conduction electrons. It should be noted that all the results of Secs. II A and II B are further reduced to the results in Sec. II C under certain limiting conditions.

II. THEORETICAL BACKGROUND

A. Quantized gate capacitance in δ-MODFEDs of III–V and related materials under low and high temperatures, whose conduction electrons obey the three band model of Kane

The energy dispersion relation for the conduction electrons in III–V, ternary, and quaternary compound semiconductors can be written following the three band model of Kane[48,49] as

$$\zeta(E) = \frac{E(E+E_g)(E+E_g+\Delta)\left(E_g+\frac{2}{3}\Delta\right)}{E_g(E_g+\Delta)\left(E+E_g+\frac{2}{3}\Delta\right)} = \frac{\hbar^2 k^2}{2m^*}, \tag{1}$$

where E is the energy of the electron measured perpendicular upward direction from the edge of the conduction band, E_g is the band gap, Δ is the isotropic spin-orbit splitting constant, $\hbar(=h/2\pi)$, h is the Planck's constant, m^* is the isotropic effective electron mass at $k=0$, k is the electron wave vector, $k^2=k_s^2+k_z^2$, and $k_s^2=k_x^2+k_y^2$.

Applying the triangular potential well approximation,[45–47] the complete electric subband structures parallel to the interface can be written using the Bohr-Sommerfeld's rule,[50–53]

$$\int_{z=0}^{z_T} k_z dz = \frac{2}{3}(a_i)^{3/2}, \tag{2}$$

where z_T is the classical turning point and a_i are the zeros of the Airy function[54] $A_i(a_i)=0$.

Under the application of an external electric field, Eq. (1) assumes the form

$$\zeta(E) - eF_s z[\zeta(E)]' = \frac{\hbar^2 k^2}{2m^*}, \tag{3}$$

in which e is the magnitude of the electron charge, F_s is the surface electric field along z direction, and the primes denote the differentiation of the differentiable functions with respect to E.

Under this condition, Eq. (2) can be written as

$$\int_{z=0}^{z_T}\left[\zeta(E) - eF_s z[\zeta(E)]' - \frac{\hbar^2 k_s^2}{2m^*}\right]^{1/2} dz = \frac{2\hbar}{3\sqrt{2m^*}}(a_i)^{3/2}, \tag{4}$$

where $z_T=\{eF_s[\zeta(E)]'\}^{-1}[\zeta(E)-(\hbar^2 k_s^2/2m^*)]$.

Equation (4) leads to the dispersion relation for the 2DEG of III–V and related substrate materials in δ-doped MODFEDs under the formalism of three band model of Kane as

$$\zeta(E) = \frac{\hbar^2 k_s^2}{2m^*} + a_i\left[\frac{\hbar e F_s[\zeta(E)]'}{\sqrt{2m^*}}\right]^{2/3}. \tag{5}$$

The electric subbands (E_i) in this case can be written as

$$\zeta(E_i) = a_i\left[\frac{\hbar e F_s[\zeta(E_i)]'}{\sqrt{2m^*}}\right]^{2/3}. \tag{6}$$

The 2D total density-of-states function in such system assumes the form

$$N(E) = \frac{m^* g_v}{\pi\hbar^2}\sum_{i=0}^{i_{\max}}\left[[\zeta(E)]' - \frac{2}{3}a_i\left(\frac{\hbar e F_s}{\sqrt{2m^*}}\right)^{2/3}\frac{[\zeta(E)]''}{\{[\zeta(E)]'\}^{1/3}}\right]H(E-E_i), \tag{7}$$

where g_v is the valley degeneracy and H is the Heaviside step function. For large values[51] of i, $a_i \to [3\pi/2(i+3/2)]^{2/3}$, in which i is the electric subband index.

Using Eq. (7), the expression of the surface electron concentration at temperature T in the n-channel inversion layers under external applied electric field can be written as

$$n_{2D} = \frac{m^* g_v k_B T}{\pi\hbar^2}\sum_{i=0}^{i_{\max}} F_0(\eta_1), \tag{8}$$

where k_B is the Boltzmann's constant, $F_j(\eta_1)$ is the Fermi-Dirac integral[55] of order j, and $\eta_1 \equiv (k_B T)^{-1}[\zeta(E_F) - a_i\{\hbar e F_s[\zeta(E_F)]'/\sqrt{2m^*}\}^{2/3}]$, in which E_F is the Fermi energy in this case.

Equation (8) gives the relation between 2D surface electron concentration in the triangular well and the applied surface electric field as

$$F_s = \frac{en_{2D}}{\varepsilon_s}, \tag{9}$$

where ε_s is the permittivity of the substrate material.

For a δ-doped MODFET, as the undoped spacer layer does not contain any charge, the electric field is constant and the potential function can be written as $\phi(z) = -F_s z$, vanishing at the heterostructure interface, $z=0$.

The Gaussian profile of the dopant atoms $N_D(z)$ from the heterostructure interface can be written as[44]

$$N_D(z) = N_0 \exp\left[-\left(\frac{z+s}{k}\right)^2\right], \tag{10}$$

in which s is the thickness of the δ-doped layer as measured from the interface, and other symbols are defined in the above reference.[44]

The doped cap layer, being made of the same material as that of the substrate, contains a positive charge density eN_c from the donors for which $\phi(z)$ assumes the form

$$\phi(z) = \frac{-eN_c}{2\varepsilon_s}(z+d+s)^2 - \left[\frac{eN_0 k}{\varepsilon_s}(z+d+s)\mathrm{erf}\left(\frac{-d}{k}\right)\right] - en_{2D}\left(\frac{z}{\varepsilon_s} - \frac{d}{\varepsilon_d}\right) - \left(\frac{eN_0 k^2}{\varepsilon_d}\right)\left\{\frac{-d}{k}\mathrm{erf}\left(\frac{-d}{k}\right) + \frac{1}{\sqrt{\pi}}\left(1 - \exp\left[\frac{-d^2}{k^2}\right]\right)\right\}, \tag{11}$$

where N_c is the dopant concentration of the cap of thickness c, d is the thickness of the undoped spacer layer as measured from the interface, ε_d is the permittivity of the δ-doped and the undoped layers, respectively, and erf is the error function.[54]

The gate voltage v_G may be written as

$$v_G = \frac{\mu_s - \mu_m}{e}, \tag{12}$$

where μ_s and μ_m are the Fermi levels of the 2DEG and the metal, respectively (all the energies and potentials being measured from the conduction band minimum of the inversion layer).

It should be noted that the Fermi level of the 2DEG is given by $E_F(n_{2D}) + \zeta(E_i)$, in which $E_F(n_{2D})$ and $\zeta(E_i)$ must be calculated from Eqs. (8) and (6), respectively, for the present case.

The Schottky barrier at the gate-surface boundary pins the conduction band E_c at the barrier voltage V_b above the metal Fermi level μ_m so that $\mu_m = -e\phi[-(c+d+s)] - V_b$, and thus,

$$\mu_m = e^2\left\{\frac{N_c c^2}{2\varepsilon_s} + N_d k\left(\frac{c}{\varepsilon_s} + \frac{d}{\varepsilon_d}\right)\mathrm{erf}\left(\frac{-d}{k}\right) + \frac{N_d k^2}{\sqrt{\pi}\varepsilon_d}\left(1 - \exp\left[\frac{-d^2}{k^2}\right]\right) - n_{2D}\left(\frac{c}{\varepsilon_s} + \frac{d}{\varepsilon_d} + \frac{s}{\varepsilon_s}\right)\right\} - V_b. \tag{13}$$

Using Eqs. (12) and (13), the gate bias equation assumes the form

$$v_G = \frac{E_F(n_{2D}) + \zeta(E_i)}{e} + \frac{V_b}{e} - e\left\{\frac{N_c c^2}{2\varepsilon_s} + N_d k\left(\frac{c}{\varepsilon_s} + \frac{d}{\varepsilon_d}\right)\mathrm{erf}\left(\frac{-d}{k}\right) + \frac{N_d k^2}{\sqrt{\pi}\varepsilon_d}\left[1 - \exp\left[\frac{-d^2}{k^2}\right]\right) - n_{2D}\left(\frac{c}{\varepsilon_s} + \frac{d}{\varepsilon_d} + \frac{s}{\varepsilon_s}\right)\right\}. \tag{14}$$

The gate-channel capacitance C_G can in general be written as[56,57]

$$\frac{1}{C_G} = \frac{1}{e}\frac{\partial v_G}{\partial n_{2D}}. \tag{15}$$

Using Eqs. (13) and (14), C_G in III–V and related substrate material in δ-doped MODFED under external applied electric field at temperature T can be expressed as

$$\frac{1}{C_G} = \left(\frac{c}{\varepsilon_s} + \frac{d}{\varepsilon_d} + \frac{s}{\varepsilon_s}\right) + \frac{1}{e^2}[P_1(i,E_F) + Q_1(i,E_F)], \tag{16}$$

where

$$P_1(i,E_F) \equiv \left\{\frac{m^* g_v}{\pi\hbar^2}\left[\sum_{i=0}^{i_{\max}} F_{-1}(\eta_1)\right]\left[[\zeta(E_F)]' - \left(\frac{2}{3}\right)a_i\left(\frac{\hbar e F_s}{\sqrt{2m^*}}\right)^{2/3}\frac{[\zeta(E_F)]''}{\{[\zeta(E_F)]'\}^{1/3}}\right]\right\}^{-1},$$

and

$$Q_1(i,E_F) \equiv \left(\frac{2e}{3\varepsilon_s}\right)a_i\left[\frac{\hbar e[\zeta(E_F)]'}{\sqrt{2m^*}}\right]^{2/3}(F_s)^{-1/3}$$

.

At low temperatures, most of the carriers occupy the lowest energy level[58–60] and thus, Eqs. (8) and (16) are reduced to

$$n_{2D} = \frac{m^* g_v}{\pi\hbar^2}\left[\zeta(E_F) - a_0\left\{\frac{\hbar e F_s[\zeta(E_F)]'}{\sqrt{2m^*}}\right\}^{2/3}\right], \tag{17}$$

and

$$\left.\frac{1}{C_G}\right|_{T\to 0, i=0} = \left(\frac{c}{\varepsilon_s} + \frac{d}{\varepsilon_d} + \frac{s}{\varepsilon_s}\right) + \frac{1}{e^2}[P_2(0,E_F) + Q_2(0,E_F)], \tag{18}$$

where $P_2(0,E_F) \equiv \{(m^* g_v/\pi\hbar^2)[[\zeta(E_F)]' - (2/3)a_0(\hbar e F_s/\sqrt{2m^*})^{2/3}[\zeta(E_F)]''/\{[\zeta(E_F)]'\}^{1/3}]\}^{-1}$, and $Q_2(0,E_F) \equiv ((2e/3\varepsilon_s)a_0[\hbar e[\zeta(E_F)]'/\sqrt{2m^*}]^{2/3}(F_s)^{-1/3})$.

As the electrons begin to colonize the channel, the gate bias becomes the threshold voltage (v_T). In such a case, the band becomes flat in the substrate, and the spacer reduces the Fermi and subband energies to zero, leading to the expression of v_T as,

$$v_T = \frac{V_b}{e} - e\left\{\frac{N_c c^2}{2\varepsilon_s} + N_d k\left(\frac{c}{\varepsilon_s} + \frac{d}{\varepsilon_d}\right)\mathrm{erf}\left(-\frac{d}{k}\right) + \frac{N_d k^2}{\sqrt{\pi}\varepsilon_d}(1 - e^{-d^2/k^2})\right\}. \quad (19)$$

B. Quantized gate capacitance in δ-MODFEDs of III–V and related materials under low and high temperatures, whose conduction electrons obey the two band model of Kane

Under the condition $\Delta \gg E_g$ or $\Delta \ll E_g$, Eq. (1) can be written as

$$E(1 + \alpha E) = \frac{\hbar^2 k^2}{2m^*}, \quad (20)$$

where α is the non-parabolicity parameter and is approximately given by[48,49] $1/E_g$. Equation (20) is commonly known as the two band model of Kane.[48,49]

Proceeding similarly, the dispersion relation in this case assumes the form

$$E(1 + \alpha E) = \frac{\hbar^2 k_s^2}{2m^*} + a_i\left[\frac{\hbar e F_s(1 + 2\alpha E)}{\sqrt{2m^*}}\right]^{2/3}. \quad (21)$$

Equation (21) under the influence of an externally applied electric field is well known in literature.[61]

The subband energies, total density-of-states function, and the carrier concentration can respectively be written as

$$E_i(1 + \alpha E_i) = a_i\left[\frac{\hbar e F_s(1 + 2\alpha E_i)}{\sqrt{2m^*}}\right]^{2/3}, \quad (22)$$

$$N(E) = \frac{m^* g_v}{\pi\hbar^2}\sum_{i=0}^{i_{\max}}\left\{(1 + 2\alpha E) - \frac{2}{3}a_i\left(\frac{\hbar e F_s}{\sqrt{2m^*}}\right)^{2/3}\frac{2\alpha}{[(1 + 2\alpha E)]^{1/3}}\right\}H(E - E_i), \quad (23)$$

and

$$n_{2D} = \frac{m^* g_v k_B T}{\pi\hbar^2}\sum_{i=0}^{i_{\max}} F_0(\eta_2), \quad (24)$$

where $\eta_2 = (k_B T)^{-1}\{E_F(1 + \alpha E_F) - a_i[\hbar e F_s(1 + 2\alpha E_F)/\sqrt{2m^*}]^{2/3}\}$.

The gate bias is given by Eq. (14), in which $E_F(n_{2D})$ should be determined from Eq. (24) in this case. Using Eqs. (16) and (24), C_G in III–V and related substrate material in δ-doped MODFED under external applied electric field at temperature T in this case can be expressed as

$$\frac{1}{C_G} = \left(\frac{c}{\varepsilon_s} + \frac{d}{\varepsilon_d} + \frac{s}{\varepsilon_s}\right) + \frac{1}{e^2}[P_3(i, E_F) + Q_3(i, E_F)], \quad (25)$$

where

$$P_3(i, E_F) \equiv \left\{\left(\frac{m^* g_v}{\pi\hbar^2}\right)\left[\sum_{i=0}^{i_{\max}} F_{-1}(\eta_2)\right]\left\{(1 + 2\alpha E_F) - \left(\frac{2}{3}\right)a_i\left(\frac{\hbar e F_s}{\sqrt{2m^*}}\right)^{2/3}\frac{2\alpha}{[1 + 2\alpha E_F]^{1/3}}\right\}\right\}^{-1},$$

and $Q_3(i, E_F) \equiv \{(2e/3\varepsilon_s)a_i[\hbar e[(1 + 2\alpha E_F)]/\sqrt{2m^*}]^{2/3}(F_s)^{-1/3}\}$.

At low temperatures, Eqs. (24) and (25) are reduced to

$$n_{2D} = \frac{m^* g_v}{\pi\hbar^2}\left\{E_F(1 + \alpha E_F) - a_0\left[\frac{\hbar e F_s(1 + 2\alpha E_F)}{\sqrt{2m^*}}\right]^{2/3}\right\}, \quad (26)$$

and

$$\left.\frac{1}{C_G}\right|_{T\to 0, i=0} = \left(\frac{c}{\varepsilon_s} + \frac{d}{\varepsilon_d} + \frac{s}{\varepsilon_s}\right) + \frac{1}{e^2}[P_4(0, E_F) + Q_4(0, E_F)], \quad (27)$$

in which $P_4(0, E_F) \equiv \{(m^* g_v/\pi\hbar^2)\{(1 + 2\alpha E_F) - (2/3)a_0(\hbar e F_s/\sqrt{2m^*})^{2/3}2\alpha/[(1 + 2\alpha E_F)]^{1/3}\}\}^{-1}$, and $Q_4(0, E_F) \equiv \{(2e/3\varepsilon_s)a_0[\hbar e(1 + 2\alpha E_F)/\sqrt{2m^*}]^{2/3}(F_s)^{-1/3}\}$.

C. Quantized gate capacitance in δ-MODFEDs of III–V and related materials under low and high temperatures, whose conduction electrons obey the parabolic energy band model

For wide gap materials, Eqs. (19) and (20) are reduced to

$$E = \frac{\hbar^2 k^2}{2m^*}. \quad (28)$$

Equation (28) is known as the parabolic energy band model of Kane.[48,49]

The dispersion relation following Eq. (2) under the application of an external electric field gets simplified as

$$E = \frac{\hbar^2 k_s^2}{2m^*} + a_i\left[\frac{\hbar e F_s}{\sqrt{2m^*}}\right]^{2/3}. \quad (29)$$

Equation (29) is well known in the literature.[45,46]

The subband energies, the total density-of-states function, and the carrier concentration can similarly be written as

$$E_i = a_i\left[\frac{\hbar e F_s}{\sqrt{2m^*}}\right]^{2/3}, \quad (30)$$

$$N(E) = \frac{m^* g_v}{\pi\hbar^2}\sum_{i=0}^{i_{\max}} H(E - E_i), \quad (31)$$

and

$$n_{2D} = \frac{m^* g_v k_B T}{\pi\hbar^2}\sum_{i=0}^{i_{\max}} F_0(\eta_3), \quad (32)$$

where $\eta_3 = (k_B T)^{-1}[E_F - a_i(\hbar e F_s/\sqrt{2m^*})^{2/3}]$.

The equation for the gate bias v_G is given by the Eq. (14), in which $E_F(n_{2D})$ should be determined from Eq. (32) for the present case.

Using the appropriate equations, C_G in III–V and related substrate materials in δ-doped MODFED under external applied electric field at temperature T assumes the well known form

$$\frac{1}{C_G} = \left(\frac{c}{\varepsilon_s} + \frac{d}{\varepsilon_d} + \frac{s}{\varepsilon_s}\right) + \frac{1}{e^2}[P_5(i,E_F) + Q_5(i,E_F)], \tag{33}$$

where $P_5(i,E_F) \equiv \left\{\left(m^* g_v / \pi\hbar^2\right)\left(\sum_{i=0}^{i_{\max}} F_{-1}(\eta_3)\right)\right\}^{-1}$ and $Q_5(i,E_F) \equiv \{(2e/3\varepsilon_s)a_i[\hbar e/\sqrt{2m^*}]^{2/3}(F_s)^{-1/3}\}$.

At low temperatures, Eq. (32) reduces to

$$n_{2D} = \frac{m^* g_v}{\pi\hbar^2}\left[E_F - a_0\left(\frac{\hbar e F_s}{\sqrt{2m^*}}\right)^{2/3}\right]. \tag{34}$$

Assuming that the lowest subband is occupied, the gate bias in Eq. (14) gets simplified as

$$v_G = \frac{e n_{2D}}{\varepsilon_s}\frac{r_B}{4} + 2\frac{a_0}{e}\left[\frac{\hbar e F_s}{\sqrt{2m^*}}\right]^{2/3} + \frac{V_b}{e} - e\left\{\frac{N_c c^2}{2\varepsilon_s} + N_d k\left(\frac{c}{\varepsilon_s} + \frac{d}{\varepsilon_d}\right)\mathrm{erf}\left(-\frac{d}{k}\right) + \frac{N_d k^2}{\sqrt{\pi}\varepsilon_d}(1 - e^{-d^2/k^2}) - n_{2D}\left(\frac{c}{\varepsilon_s} + \frac{d}{\varepsilon_d} + \frac{s}{\varepsilon_s}\right)\right\}, \tag{35}$$

where r_B is the scaled Bohr radius.

The gate-channel capacitance thus reduces to

$$\left.\frac{1}{C_G}\right|_{T\to 0, i=0} = \left(\frac{c}{\varepsilon_s} + \frac{d}{\varepsilon_d} + \frac{s}{\varepsilon_s}\right) + \left\{\frac{r_B}{4\varepsilon_s} + \frac{4}{3n_{2D}^{1/3}}a_0\left(\frac{\hbar e^2}{\sqrt{2m^*\varepsilon_s}}\right)^{2/3}\right\}. \tag{36}$$

III. RESULT AND DISCUSSIONS

Using Table I and the appropriate equations, in Fig. 1, the gate capacitance per unit area has been plotted as function of the surface electric field at $T=300$ K for $Al_xGa_{1-x}As|GaAs$ δ-doped MODFED, whose 2DEG follows the three, two, and the parabolic energy band models of Kane. The relative shift of the gate capacitance clearly exhibits the significant dependence of the same on the spectrum constants of the 2DEG in the n-channel inversion layer. The application of such high values of the surface electric field on the 2DEG results the formation of the electric subbands, which signatures the quantization of the motion of the carriers and hence the quantized Fermi energies. The contribution of the electric subbands on the gate capacitance significantly enhances its value. It should be noted that the value of the gate capacitance in δ-doped MODFED is considerably less than the corresponding cases of bulk MOS devices since the gate bias affects the density of the carriers in the triangular well, reducing them to zero. This results in lowering of the net amount of charge at the interface and hence lowering the interface quantum capacitance contribution to the overall gate capacitance. In addition, as the spacer layer in MODFED spatially separates the impurities and the 2DEG, the mobility is higher in such devices and finds extensive applications as modern high electron mobility transistors.

In Fig. 2, the gate capacitance per unit area has been plotted as function of the gate voltage for all the cases of Fig. 1. The influence of quantum confinement is immediately apparent from all the figures since the gate capacitance depends strongly on the quantized energies of the 2DEG, which is in direct contrast with their respective bulk devices. With higher values of the surface electric field, the carrier degeneracy in the strongly inverted n-channel increases, thereby increasing the gate capacitance. It appears that the gate capacitance follows a steplike behavior although the numerical

TABLE I. Values of the energy band constants and device parameters.

(a) InSb:[a,b] $E_g=0.2352$ eV, $\Delta=0.81$ eV, $m^*=0.01359m_0$, $\varepsilon_s=16.8\varepsilon_0$ (ε_0 is the permittivity of free space), $g_v=1$, and $V_b=0.2$ eV
(b) $Al_{0.4}In_{0.6}Sb$:[c] $\varepsilon_s=15.65\varepsilon_0$
(c) n-GaAs:[a,d] $E_g=1.55$ eV, $\Delta=0.35$ eV, $m^*=0.07m_0$, $g_v=1$, and $V_b=0.7$ eV
(d) $Al_{0.4}Ga_{0.6}As$:[e] $\varepsilon_s=11.9\varepsilon_0$
(e) $In_{0.906}Ga_{0.094}As_{0.2}P_{0.8}$:[a,f] $E_g=1.19$ eV, $\Delta=0.1572$ eV, $m^*=0.0722m_o$, $g_v=1$, and $V_b=0.6$ eV
(f) $In_{0.52}Al_{0.48}As$:[g] $\varepsilon_s=11.6\varepsilon_0$
(g) Cap thickness:[h] 5 nm
(h) Dopant thickness:[h] 10 nm
(h) Spacer thickness:[h] 5 nm
(i) k is a selected constant to fit the real δ distribution[i]

[a]Reference 62.
[b]Reference 63.
[c]Reference 64.
[d]Reference 57.
[e]Reference 65.
[f]Reference 66.
[g]Reference 67.
[h]Reference 68.
[i]Reference 44.

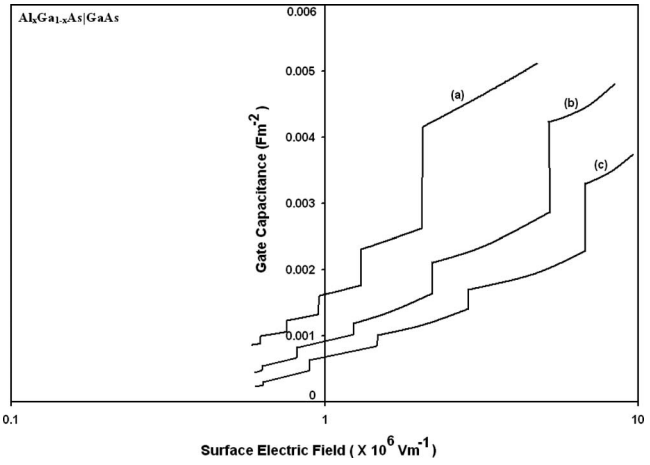

FIG. 1. The plot of the gate capacitance at $T=300$ K as a function of surface electric field for the n-channel inversion layers in $Al_xGa_{1-x}As|GaAs$ δ-doped MODFED in which the curves (a)–(c) represent the parabolic, the two, and the three band energy models of Kane ($N_0=1.0\times10^{24}$ m^{-3}, $N_c=1.0\times10^{23}$ m^{-3}).

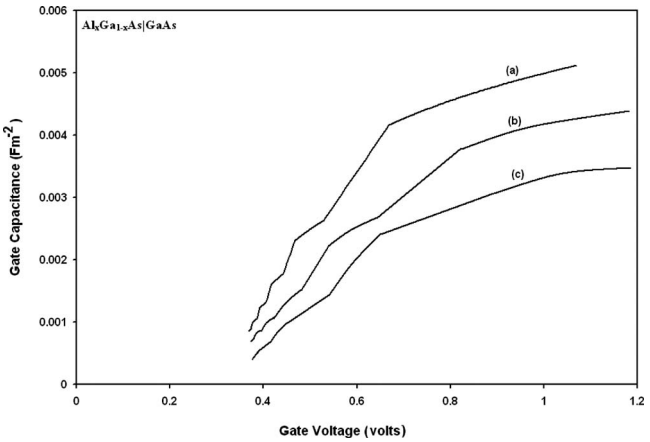

FIG. 2. The plot of the gate capacitance at $T=300$ K as a function of gate voltage for the n-channel inversion layers in $Al_xGa_{1-x}As|GaAs$ δ-doped MODFED in which the curves (a)–(c) represent the parabolic, the two, and the three band energy models of Kane ($N_0=1.0\times10^{24}$ m^{-3}, $N_c=1.0\times10^{23}$ m^{-3}).

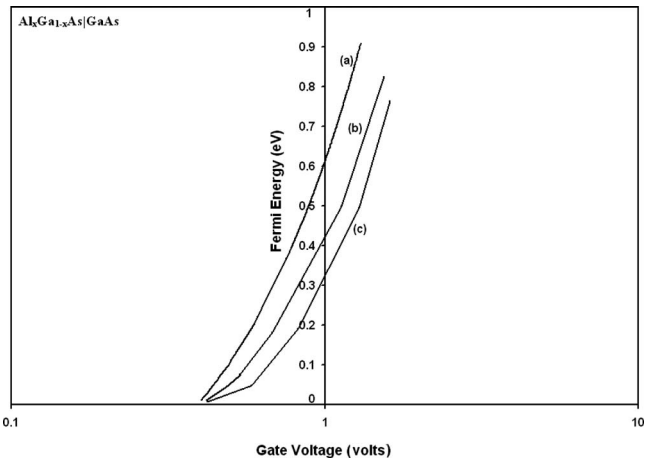

FIG. 4. The plot of the Fermi energy at $T=300$ K as a function of gate voltage for the n-channel inversion layers in $Al_xGa_{1-x}As|GaAs$ δ-doped MODFED in which the curves (a)–(c) represent the parabolic, the two, and the three band energy models of Kane ($N_0=1.0\times10^{24}$ m^{-3}, $N_c=1.0\times10^{23}$ m^{-3}).

values vary widely and are determined by the constants of the energy spectra. The oscillatory dependence is due to the crossing over of the Fermi level by the quantized levels. For each coincidence of such levels with the Fermi level, there would be a discontinuity in the density-of-states function resulting in a sudden jump in magnitude. It should be noted that the height of step size and the rate of decrement are totally dependent on the band structure of the 2DEG. Figures 3 and 4 exhibit the plot of the Fermi energy as functions of surface electric field, and the gate bias for $Al_xGa_{1-x}As|GaAs$ δ-doped MODFED at $T=300$ K. The reason for increase in the Fermi energy with the applied field and bias follows the discussion from the previous part.

Although, an extensive work has been done for $Al_xGa_{1-x}As|GaAs$, other III–V MODFEDs such as $Al_xIn_{1-x}Sb|InSb$ (Ref. 16) and $In_{1-x}Al_xAs|In_{1-x}Ga_xAs_yP_{1-y}$ lattices matched to InP (Refs. 69–71) have also been reported in literature. It appears that the theoretical investigations on quantized gate capacitance for such devices have been less reported although such structures find many extensive applications in high mobility systems since the band gap of these optoelectronic materials can be varied over a wide range by adjusting the alloy composition.[72] These compounds can be extremely useful and are widely investigated because of their significant enhancement of carrier mobility[73] and low effective mass.[64] Hence, the use of such compounds may have a great impact on the nanoscale transistor technologies. What follows, in Figs. 5–12, the gate capacitance and the Fermi energy have been plotted as functions of applied electric field and gate bias, respectively, whose conduction electrons in the channel follows the three, two, and the parabolic energy band models of Kane.[48,49] It appears from all the figures that the gate capacitance is the largest for $Al_xGa_{1-x}As|GaAs$ and the least for $Al_xIn_{1-x}Sb|InSb$.

For a condensed paper presentation, the influences of the quantization and the defect centers due to the alloy composition (DX centers) on threshold voltage have been ne-

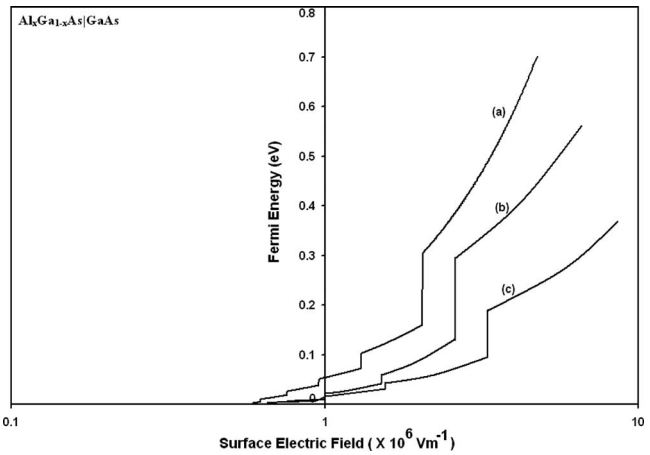

FIG. 3. The plot of the Fermi energy at $T=300$ K as a function of surface electric field for the n-channel inversion layers in $Al_xGa_{1-x}As|GaAs$ δ-doped MODFED in which the curves (a)–(c) represent the parabolic, the two, and the three band energy models of Kane ($N_0=1.0\times10^{24}$ m^{-3}, $N_c=1.0\times10^{23}$ m^{-3}).

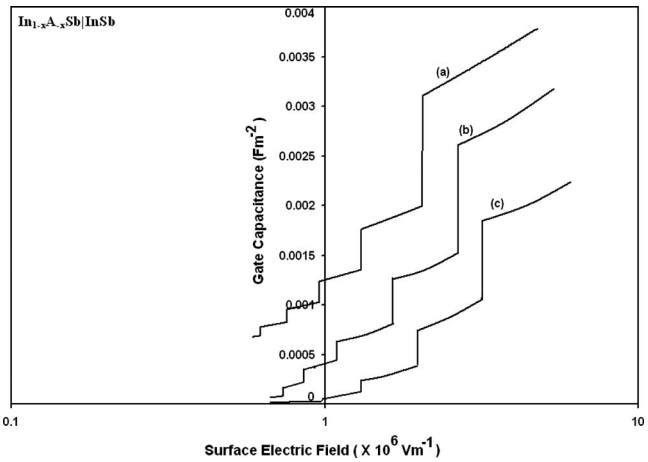

FIG. 5. The plot of the gate capacitance at $T=300$ K as a function of surface electric field for the n-channel inversion layers in $In_{1-x}As_{-x}Sb|InSb$ δ-doped MODFED in which the curves (a)–(c) represent the parabolic, the two, and the three band energy models of Kane ($N_0=1.0\times10^{24}$ m^{-3}, $N_c=1.0\times10^{23}$ m^{-3}).

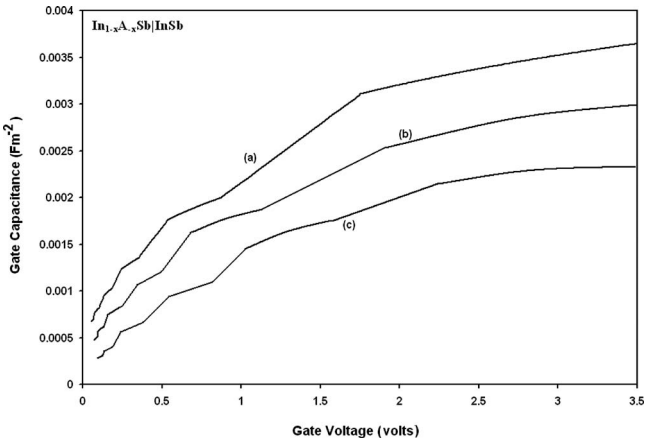

FIG. 6. The plot of the gate capacitance at $T=300$ K as a function of gate voltage for the n-channel inversion layers in $In_{1-x}As_{-x}Sb|InSb$ δ-doped MODFED in which the curves (a)–(c) represent the parabolic, the two, and the three band energy models of Kane ($N_0=1.0\times10^{24}$ m^{-3}, $N_c=1.0\times10^{23}$ m^{-3}).

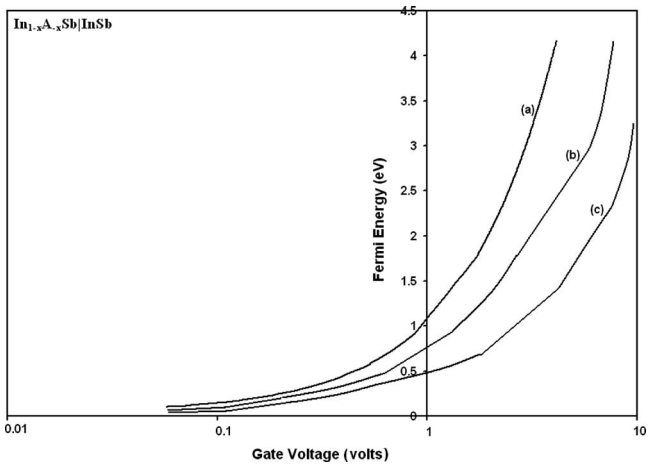

FIG. 8. The plot of the Fermi energy at $T=300$ K as a function of gate voltage for the n-channel inversion layers in $In_{1-x}As_{-x}Sb|InSb$ δ-doped MODFED in which the curves (a)–(c) represent the parabolic, the two, and the three band energy models of Kane ($N_0=1.0\times10^{24}$ m^{-3}, $N_c=1.0\times10^{23}$ m^{-3}).

glected, which can significantly affect its value.[74,75] Such incorporation would certainly enhance the accuracy of our results on the threshold voltage. The values of the gate capacitances and the Fermi energies after proper inclusion of the subband energies for respective MODFED at room temperature can be compared with the available data for relative comparison. Our method is not at all related to the density-of-states technique as used in literature[76] since, from the **E**-**k** dispersion relation, one can obtain the DOS. However, the DOS technique as used in literature[76] cannot provide the **E**-**k** dispersion relation. Therefore, our study is more fundamental than those existing in the literature since the Boltzmann transport equation, which controls the study of the charge transport properties of semiconductor devices, can be solved if and only if the **E**-**k** dispersion relation is known. It may be remarked that, in recent years, the carrier statistics of III–V and related materials have been extensively studied[77,78] yet the quantized gate capacitance for the n-channel inversion layers in MODFEDs have been less investigated by considering the band non-parabolicity of the channel materials. We wish to note that we have not considered the hot electron and many body effects in this simplified theoretical formalism due to the lack of proper analytical techniques in the literature for including them in the present system. Our simplified approach will be useful for the purpose of comparison when methods for tackling the formidable problem after inclusion of such effects for the present generalized systems would appear. The inclusion of the aforesaid effects would certainly increase the accuracy of our results although the qualitative features of the quantized gate capacitance, as discussed here, would not change in the presence of the aforementioned effects.

While formulating our results, we have assumed that the potential well at the surface may be approximated by a triangular well, which however, introduces some errors such as negligence of the free charge contribution to the potential. This kind of approach is reasonable if there are only a few

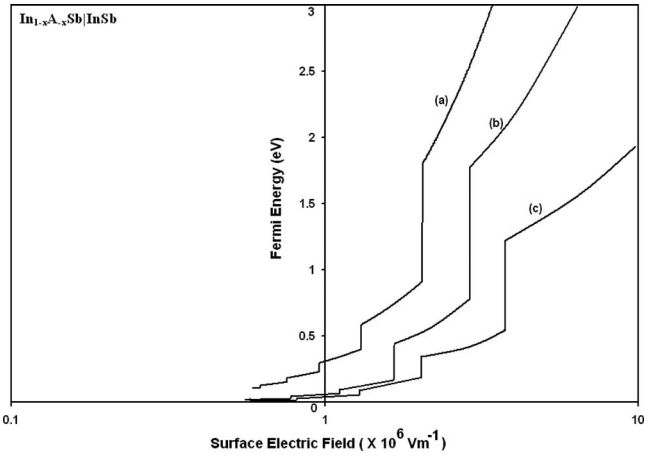

FIG. 7. The plot of the Fermi energy at $T=300$ K as a function of surface electric field for the n-channel inversion layers in $In_{1-x}As_{-x}Sb|InSb$ δ-doped MODFED in which the curves (a)–(c) represent the parabolic, the two, and the three band energy models of Kane ($N_0=1.0\times10^{24}$ m^{-3}, $N_c=1.0\times10^{23}$ m^{-3}).

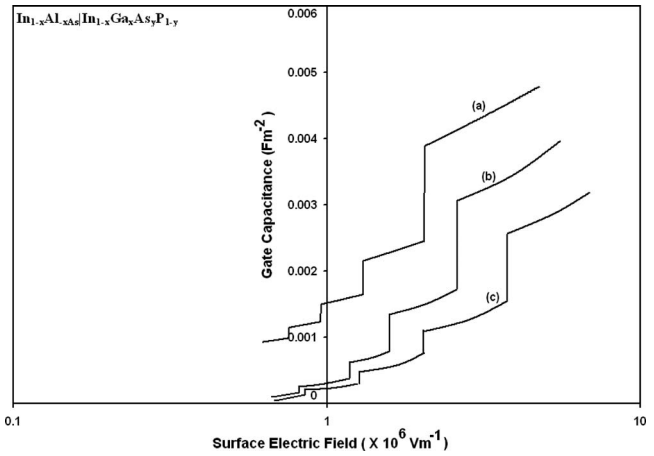

FIG. 9. The plot of the gate capacitance at $T=300$ K as a function of surface electric field for the n-channel inversion layers in $In_{1-x}Al_{-x}As|In_{1-x}Ga_xAs_yP_{1-y}$ δ-doped MODFED in which the curves (a)–(c) represent the parabolic, the two, and the three band energy models of Kane ($N_0=1.0\times10^{24}$ m^{-3}, $N_c=1.0\times10^{23}$ m^{-3}).

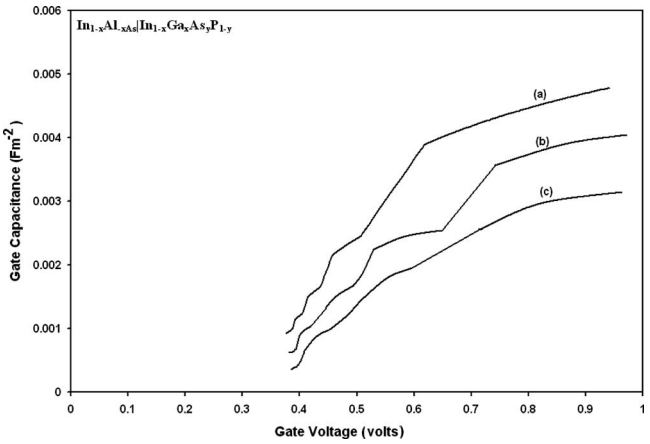

FIG. 10. The plot of the gate capacitance at $T=300$ K as a function of gate voltage for the n-channel inversion layers in $In_{1-x}Al_{-x}As|In_{1-x}Ga_xAs_yP_{1-y}$ δ-doped MODFED in which the curves (a)–(c) represent the parabolic, the two, and the three band energy models of Kane ($N_0=1.0\times10^{24}$ m^{-3}, $N_c=1.0\times10^{23}$ m^{-3}).

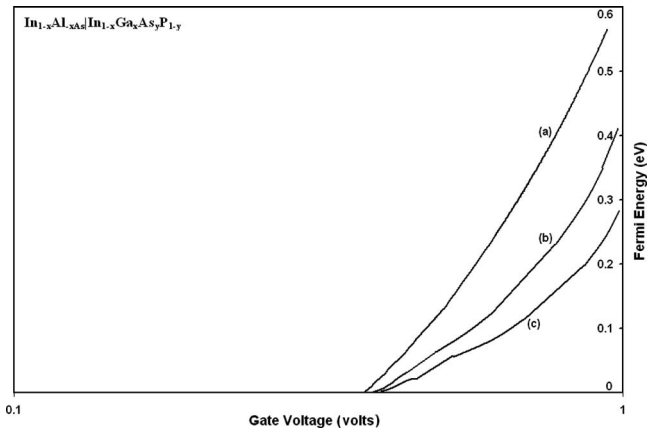

FIG. 12. The plot of the Fermi energy at $T=300$ K as a function of gate voltage for the n-channel inversion layers in $In_{1-x}Al_{-x}As|In_{1-x}Ga_xAs_yP_{1-y}$ δ-doped MODFED in which the curves (a)–(c) represent the parabolic, the two, and the three band energy models of Kane ($N_0=1.0\times10^{24}$ m^{-3}, $N_c=1.0\times10^{23}$ m^{-3}).

charge carriers in the inversion layer but is responsible for an overestimation of the splitting when the inversion carrier density exceeds that of the depletion layer. This approximation will not introduce significant error since, for actual calculations, one needs to solve both Schrödinger's and Poisson's equations self-consistently, which is a formidable problem for the present generalized system due to the nonavailability of the proper analytical techniques, without exhibiting a widely different qualitative behavior.[45] The second assumption deals with the analyses of the numerical calculations in electric quantum limit where the quantum effects become prominent. The errors that are being introduced for these assumptions will not affect too much the results at low temperatures.[79] Hence, for electric quantum limit, the temperature has been assumed to be low since, in that case, most of the electrons are at the lowest electric subband.[58–60,79] We have not considered other types of optoelectronic materials and other external variables in order to keep the presentation brief. Besides, the influence of energy band models and the various band constants on the gate capacitances for different MODFEDs made of III–V, II–VI, IV–VI, and related ternary substrates can also be estimated from all the figures.

Thus, we have presented an analytical expression of the quantized gate capacitance in different MODFEDs by including proper quantum mechanical treatment on the band non-parabolicity of the substrates. It should be noted that the quantum capacitance is an inherent property of 2DEG system.[80] Under certain limiting conditions, the respective generalized expressions, as derived here for the parabolic energy dispersion model, reduce to the results in confirmation with Pal *et al.*[81] The theoretical results as given here would be useful in analyzing various other experimental data[82] related to this phenomenon. Finally, it may be concluded that this theory can also be used to investigate the gate capacitances, Burstien-Moss shift, the effective electron mass, the specific heat, and other different transport coefficients of modern ultrathin film semiconductor devices operated under the influence of external photon field.

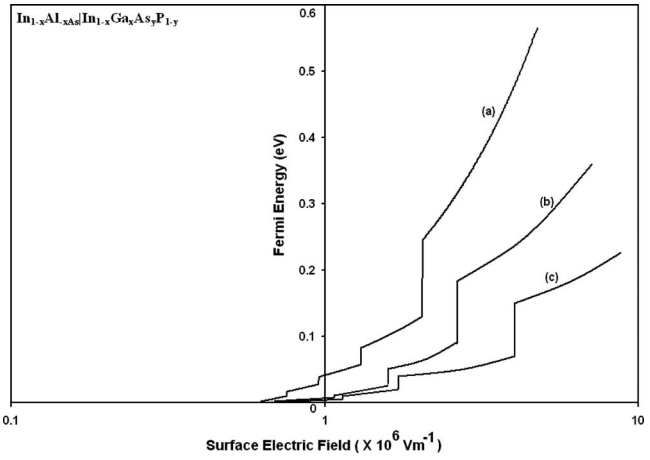

FIG. 11. The plot of the Fermi energy at $T=300$ K as a function of surface electric field for the n-channel inversion layers in $In_{1-x}Al_{-x}As|In_{1-x}Ga_xAs_yP_{1-y}$ δ-doped MODFED in which the curves (a)–(c) represent the parabolic, the two, and the three band energy models of Kane ($N_0=1.0\times10^{24}$ m^{-3}, $N_c=1.0\times10^{23}$ m^{-3}).

[1] T. Sugaya, T. Yamane, M. Ogura, K. Komori, and K. Yonei, J. Cryst. Growth **278**, 94 (2005).
[2] Y. Wang and S. Y. Chou, Appl. Phys. Lett. **63**, 2257 (1993).
[3] D. Ramamurthy and C. H. Wu, Phys. Rev. B **66**, 115307 (2002).
[4] S. Amaha, T. Hatano, S. Teraoka, A. Shibatomi, S. Tarucha, Y. Nakata, T. Miyazawa, T. Oshima, T. Usuki, and N. Yokoyama, Appl. Phys. Lett. **92**, 202109 (2008).
[5] S.-T. Cheng and C.-Y. Wang, IEEE Trans. Circuits Syst., I: Regul. Pap. **53**, 316 (2006).
[6] T. van Zoest, T. Müller, T. Wendrich, M. Gilowski, E. M. Rasel, T. Könemann, C. Lämmerzahl, H. J. Dittus, A. Vogel, K. Bongs, K. Sengstock, W. Lewoczko, and A. Peters, Proc. SPIE **6483**, 648306 (2007).
[7] G. K. Brennen, C. M. Caves, P. S. Jessen, and I. H. Deutsch, Phys. Rev. Lett. **82**, 1060 (1999).
[8] L. Liao, A. Liu, D. Rubin, J. Basak, Y. Chetrit, H. Nguyen, R. Cohen, N. Izhaky, and M. Paniccia, Electron. Lett. **43**, 1196 (2007).
[9] K. E. Stubkjaer, Proceedings of the International Conference Optical Switching Systems Using Nanostructures; Lasers and Electro-Optics, (CLEO), 2004 (unpublished), Vol. 2, p. 2.
[10] A. Cho and H. Casey, IEEE J. Quantum Electron. **10**, 791 (1974).
[11] S. Nagata, T. Tanaka, and M. Fukai, Appl. Phys. Lett. **30**, 503 (1977).
[12] S. Harrer, S. Strobel, G. Scarpa, G. Abstreiter, M. Tornow, and P. Lugli, IEEE Trans. Nanotechnol. **7**, 363 (2008).
[13] A. Tukiainen, L. Toikkanen, M. Haavisto, V. Erojrvi, V. Rimpilinen, J. Viheril, and M. Pessa, IEEE Photonics Technol. Lett. **18**, 2257 (2006).

[14]S.-G. Ihn, J.-I. Song, Y.-H. Kim, J. Y. Lee, and I.-H. Ahn, IEEE Trans. Nanotechnol. **6**, 384 (2007).
[15]R. Dingle, H. L. Stormer, A. C. Gossard, and W. Wiegmann, Appl. Phys. Lett. **33**, 665 (1978).
[16]S. Datta, Microelectron. Eng. **84**, 2133 (2007).
[17]R. Chau, S. Datta, M. Doczy, B. Doyle, B. Jin, J. Kavalieros, A. Majumdar, M. Metz, and M. Radosavljevic, IEEE Trans. Nanotechnol. **4**, 153 (2005).
[18]T. Ashley, L. Buckle, S. Datta, M. T. Emeny, D. G. Hayes, K. P. Hilton, R. Jefferies, T. Martin, T. J. Phillips, D. J. Wallis, P. J. Wilding, and R. Chau, Electron. Lett. **43**, 777 (2007).
[19]J. S. Moon, W. Shihchang, D. Wong, I. Milosavljevic, A. Conway, P. Hashimoto, M. Hu, M. Antcliffe, and M. Micovic, IEEE Electron Device Lett. **26**, 348 (2005).
[20]Y. Cai, K. J. Chen, and K. M. Lauet, IEEE Electron Device Lett. **26**, 435 (2005).
[21]K. Hikosaka, S. Sasa, N. Harada, and S. Kurodaet, IEEE Electron Device Lett. **9**, 241 (1988).
[22]I. Thayne, M. Holland, Y.C. Chen, W.Q. Li, A. Paulsen, S. Beaumont, and P. Bhattacharya, Tech. Dig. - Int. Electron Devices Meet. **225** (1993).
[23]T. Enoki, M. Tomizawa, Y. Umeda, and Y. Ishii, Jpn. J. Appl. Phys., Part 1 **33**, 798 (1994).
[24]K. Shinohara, Y. Yamashita, A. Endoh, K. Hikosaka, T. Matsui, T. Mimura, and S. Hiyamizu, Jpn. J. Appl. Phys., Part 1 **41**, 437 (2002).
[25]W. Kruppa, J. B. Boos, B. R. Bennett, N. A. Papanicolaou, D. Park, and R. Bass, Electron. Lett. **42**, 688 (2006).
[26]Z. H. Feng, J. Y. Yin, F. P. Yuan, B. Liu, Z. Feng, and S. J. Cai, Proc. SPIE **6984**, 698435 (2008).
[27]R. Chau, S. Datta, and A. Majumdar, Proceedings of the IEEE CSIC Digest, 2005 (unpublished).
[28]F. Koch, A. Zrenner, and M. Zachau, in *Two Dimensional Systems: Physics and New Devices*, Series in Solid State Science Vol. 67, edited by G. Bauer, F. Kucher, and H. Heinrich (Springer, New York, 1986), p. 175.
[29]S. J. Koester, J. O. Chu, and C. S. Webster, Electron. Lett. **36**, 674 (2000).
[30]H. Leier, A. Vescan, R. Dietrich, A. Wieszt, and H. Tobler, Proceedings of the IEE Digest, 1999 (unpublished), Vol. 4, p. 1999.
[31]Y. H. Lo, M. Bagheri, P. S. D. Lin, P. Grabbe, R. Bhat, N. G. Stoffel, T. P. Lee, and D. T. Kong, Electron. Lett. **26**, 807 (1990).
[32]P. Valizadeh, D. Pavlidis, K. Shiojima, T. Makimura, and N. Shigekawa, Solid-State Electron. **49**, 1352 (2005).
[33]M. J. Rack, T. J. Thornton, D. K. Ferry, J. Huffman, and R. Westhoff, Solid-State Electron. **45**, 1199 (2001).
[34]J. J. Rosenberg, M. Benlamri, P. D. Kirchner, J. M. Woodall, and G. D. Pettit, IEEE Electron Device Lett. **6**, 491 (1985).
[35]B. Pereiaslavets, G. H. Martin, L. F. Eastman, R. W. Yanka, J. M. Ballingall, J. Braunstein, K. H. Bachem, and B. K. Ridley, IEEE Trans. Electron Devices **44**, 1341 (1997).
[36]T. Henderson, M. I. Aksun, C. K. Peng, H. Morkoq, P. C. Chao, P. M. Smith, K.-H. G. Duh, and L. F. Lester, IEEE Electron Device Lett. **7**, 649 (1986).
[37]J. Mateos, B. G. Vasallo, D. Pardo, T. González, J. S. Galloo, Y. Roelens, S. Bollaert, and A. Cappy, Nanotechnology **14**, 117 (2003).
[38]J. I. Nishizawa, P. Plotka, and T. Kurabayashi, IEEE Trans. Electron Devices **49**, 1102 (2002).
[39]L. D. Nguyen, "Realization of Ultra-High-Speed Field Effect Transistors," Ph.D. thesis, Cornell University, 1989.
[40]H. Morkoc, H. Unlu, and G. Ji, *Principles and Technology of MODFET's* (Wiley, New York, 1991), and references cited therein.
[41]E. F. Schubert, A. Fischer, and K. Ploog, IEEE Trans. Electron Devices **33**, 625 (1986).
[42]S. L. G. Chu, J. C. Huang, A. Bertand, M. J. Schindler, W. Struble, R. Binder, and W. Hoke, Proceedings of the IEEE GaAs IC Symposium Technical Digest, 1992 (unpublished), p. 221.
[43]R. E. Williams and D. W. Shaw, Electron. Lett. **13**, 408 (1977).
[44]M.-J. Kao, H.-M. Shieh, W.-C. Hsu, T.-Y. Lin, Y.-H. Wu, and R.-T. Hsu, IEEE Trans. Electron Devices **43**, 1181 (1996).
[45]T. Ando, A. B. Fowler, and F. Stern, Rev. Mod. Phys. **54**, 437 (1982).
[46]F. Stern and W. E. Howard, Phys. Rev. **163**, 816 (1967).
[47]W. Zawadzki, **16**, 229 (1983).
[48]E. O. Kane, J. Phys. Chem. Solids **1**, 249 (1957).
[49]B. R. Nag, *Electron Transport in Compound Semiconductors* (Springer-Verlag, Berlin, 1980).
[50]T. Fiedler, Ph.D. Thesis, Technische Hochschule Ilmenau, 1984.
[51]G. Paasch, T. Fiedler, M. Kolar, and I. Bartos, Phys. Status Solidi B **118**, 641 (1983).
[52]J.-P. Zollner, H. Ubensee, G. Paasch, T. Fiedler, and G. Gobsch, Phys. Status Solidi B **134**, 837 (1986).
[53]J.-P. Zollner and G. Paasch, Phys. Status Solidi B **151**, 145 (1989).
[54]M. Abramowitz and I. A. Stegun, *Handbook of Mathematical Functions* (Verlag, Harry, Deutsch, Frankfurt am Main, 1984).
[55]J. S. Blackmore, *Semiconductor Statistics* (Pergamon, Oxford, 1962).
[56]P. Roblin and H. Rhodin, *High Speed Heterostructure Devices: From Device Concept to Circuit Modeling* (Cambridge University Press, Cambridge, England, 2006).
[57]J. H. Davies, *Physics of Low Dimensional Semiconductors* (Cambridge University Press, Cambridge, England, 1996).
[58]S. Datta, *Electron Transport in Mesoscopic Systems* (Cambridge University Press, Cambridge, England, 1997).
[59]M. Lundstrom and J. Guo, *Nanoscale Transistors* (Springer, New York, 2006).
[60]M. Lundstrom, *Fundamentals of Carrier Transport* (Cambridge University Press, Cambridge, England, 2000).
[61]G. A. Antcliffe, R. T. Bate, and R. A. Reynolds, Proceedings of the International Conference on Physics of Semi-Metals and Narrow-Gap Semiconductors, edited by D. L. Carter and R. T. Bate (Pergamon, Oxford, 1971), p. 499.
[62]O. Madelung, *Semiconductors: Data Handbook*, 3rd ed. (Springer, New York, 2004).
[63]J. M. S. Orr, P. D. Buckle, M. Fearn, P. J. Wilding, C. J. Bartlett, M. T. Emeny, L. Buckle, and T. Ashley, Semicond. Sci. Technol. **21**, 1408 (2006).
[64]S. Adachi, *GaAs and Related Materials: Bulk Semiconducting and Superlattice Properties* (World Scientific, Singapore, 1994).
[65]S. Adachi, J. Appl. Phys. **58**, R1 (1985).
[66]J. S. Escher, L. W. James, R. Sankaran, G. A. Antypas, R. L. Moon, and R. L. Bell, J. Vac. Sci. Technol. **13**, 874 (1976).
[67]K. J. Nash, M. S. Skolnick, and S. J. Bass, Semicond. Sci. Technol. **2**, 329 (1987).
[68]Y. Jin, Solid-State Electron. **34**, 117 (1991).
[69]W. P. Hong, R. Bhat, J. R. Hayes, C. Nguyen, M. Koza, and G. K. Chang, IEEE Electron Device Lett. **12**, 559 (1991).
[70]L. Aina, M. Durgess, M. Motingly, J. M. O'Conner, A. Meerschaert, M. Tong, A. Ketterson, and A. Adesida IEEE Electron Device Lett. **12**, 483 (1991).
[71]*Optoelectronic Integration: Physics, Technology and Application*, edited by O. Wada (Springer, New York, 1994).
[72]J. Singh, *Semiconductor Optoelectronics: Physics and Technology* (McGraw-Hill, New York, 1995).
[73]N. T. Linch, Festkoerperprobleme **23**, 227 (1985).
[74]G. Chindalore, S. A. Hareland, S. Jallepalli, A. F. Tasch, Jr., C. M. Maziar, V. K. F. Chia, and S. Smith, IEEE Electron Device Lett. **18**, 206 (1997).
[75]A. Chandra and M. C. Foisy, IEEE Trans. Electron Devices **38**, 1238 (1991).
[76]J. N. Schulman and Y. C. Chang, Phys. Rev. B **24**, 4445 (1981).
[77]P. K. Chakraborty, S. Bhattacharya, and K. P. Ghatak, J. Appl. Phys. **98**, 053517 (2005).
[78]K. P. Ghatak, S. Bhattacharya, S. Bhowmik, R. Benedictus, and S. Choudhury, J. Appl. Phys. **103**, 094314 (2008).
[79]Z. A. Weinberg, Solid-State Electron. **20**, 11 (1977).
[80]S. Luryi, Appl. Phys. Lett. **52**, 501 (1988).
[81]H. S. Pal, K. D. Cantley, S. S. Ahmed, and M. S. Lundstrom, IEEE Trans. Electron Devices **55**, 904 (2008).
[82]M. Zhu, A. Usher, A. J. Matthews, A. Potts, M. Elliott, W. G. H. Harker, D. A. Ritchie, and M. Y. Simmons, Phys. Rev. B **67**, 155329 (2003).